DOI: 10.1002/cphc.200600199

Excited-State Properties and Environmental Effects for Protonated Schiff Bases: A Theoretical Study**

Adélia J. A. Aquino,* Mario Barbatti, and Hans Lischka*[a]

Complete active space self-consistent field (CASSCF), multireference configuration interaction (MRCI), density functional theory (DFT), time dependent DFT (TDDFT) and the singles and doubles coupled-cluster (CC2) methodologies have been used to study the ground state and excited states of protonated and neutral Schiff bases (PSB and SB) as models for the retinal chromophore. Systems with two to four conjugated double bonds are investigated. Geometry relaxation effects are studied in the excited $\pi\pi^*$ state using the aforementioned methods. Taking the MRCI results as reference we find that CASSCF results are quite reliable even though overshooting of geometry changes is observed. TDDFT does not reproduce bond alternation well in the $\pi\pi^*$ state. CC2 takes an intermediate position. Environmental effects due to solvent or protein surroundings have been studied in the excited states of the PSBs and SBs using a water molecule and solvated formate as model cases. Particular emphasis is given to the proton transfer process from the PSB to its solvent partner in the excited state. It is found that its feasibility is significantly enhanced in the excited state as compared to the ground state, which means that a proton transfer could be initiated already at an early step in the photodynamics of PSBs.

Introduction

Rhodopsin (Rh) and bacteriorhopsin (bR) are light sensitive proteins that have important biological functionalities. Retinal is the chromophore in both of these two proteins. In Rh, the visual cycle is initiated by photochemical isomerization of the 11-*cis*-retinal chromophore to all-*trans*-retinal when light is absorbed.[1] The photoexcitation of all-*trans*-retinal in bR leads to the formation of 13-*cis*-retinal. The initial, photochemical processes are extremely fast, occurring within a few hundred femtoseconds.[2–5] In solution, the dynamics of retinal is quite different compared to the protein environment showing biexponential decay with a shorter component which is about 20 times longer than in the protein.[6]

A large variety of quantum chemical methods have been used to study the structure and photodynamics of retinal and retinal models. The theoretical computation of the retinal photoisomerization is a difficult task because of the size of retinal and of the necessity to investigate larger sections of its excited-state energy surfaces. Moreover, as has been mentioned just above, environmental effects are very important, which require additional demanding effort for the calculations. Therefore, a wide range of theoretical investigations have been performed concentrating on various aspects of retinal ground-state and excited-state properties. Complete active space self-consistent field (CASSCF) and complete active space perturbation theory (CASPT2) are used to obtain benchmark results for vertical excitation energies and excited-state reaction paths.[7–9] The applicability of time dependent density functional theory (TDDFT) has been studied in detail,[10] in particular in view of the calculation of excited-state energy surfaces. Recently, a detailed comparison has been made between different methods including the spectroscopy oriented configuration interaction (SORCI) method, the CASSCF and CASPT2 methods.[11] Environmental effects play a crucial role for the functionality of retinal embedded in the protein pocket since they affect strongly the reactivity and spectroscopic properties of the chromophore. This has been shown by Sugihara et al.[12] and by Hufen et al.[13] for ground-state 11-*cis*-retinal embedded in a protein environment by means of density-functional dynamic simulations and by static CASSCF//CASPT2 calculations for the excited state.[14] In this work the retinal binding site has been modeled by including the Glu 113 counter ion interacting with Thr 94 and Water2b via hydrogen bonds. The DFT dynamic calculations have clearly demonstrated that the stability of the iminium group with respect to deprotonation depends significantly on the environment around Glu 113. An acetate anion has been used by Cembran et al.[15] to simulate the effect of the Glu 113 counter ion on the photochemistry of retinal. Ferre and Olivucci have probed the Rh cavity with reduced and full retinal models at the CASPT2//CASSCF/Amber level.[16,17] Extensive simulations with the Rh chromophore in the ground state has been performed by Röhrig et al.[18] using a quantum mechanical (QM) Car–Parinello dynamics in conjunction with molecular

[a] *Dr. A. J. A. Aquino, Dr. M. Barbatti, Dr. H. Lischka*
Institute for Theoretical Chemistry, University of Vienna
Waehringerstrasse 17, 1090 Vienna (Austria)
Fax: (+43) 1-4277-9527
E-mail: adelia.aquino@univie.ac.at
hans.lischka@univie.ac.at

[**] *Multireference Configuration Interaction versus Coupled Cluster and Density Functional Methods*

mechanics (MM) embedding and by Tajkhorshid et al.[19] using MM force fields. Analogous Car–Parinello QM/MM calculations have been performed by Röhrig et al.[20] for the retinal photodynamics using the restricted open-shell Kohn–Sham formalism. The photoisomerization of retinal in bR has been studied by Hayashi et al. through QM/MM calculations,[21] and proton transfer mechanisms have been investigated by Hayashi and Ohmine[22].

Even though the just-described investigations provide extensive information on the photodynamics of retinal, many important questions are still open. The reason for this can be found in the large effort required for the reliable computation of excited-state energy surfaces. Another important practical issue is the availability of analytic energy gradients and nonadiabatic coupling vectors for geometry optimizations and dynamic calculations. Up to now, a large fraction of the geometry optimizations were performed at the CASSCF level only. It is the purpose of this work to use recent advances in the calculation of multireference configuration interaction with singles and doubles (MR-CISD) analytic gradients[23–25] for obtaining reference data in particular for excited-state geometries of PSBs, which are large enough to serve as relevant benchmark systems. We also want to use our MR-CI results to assess available single-reference methods (resolution of the identity coupled cluster to second order (RI-CC2)[26,27] and time-dependent density functional theory (TDDFT)[28]) for which analytic excited-state gradients are available. These methods are clearly faster than MRCI calculations and could be used, at least, in certain domains of the energy surfaces.

The proton transfer of retinal in the ground state has already been described above (see ref. [12]). In this work we want to investigate proton transfer in the $\pi\pi^*$ excited state of PSBs and SBs. In order to model the retinal binding site we follow the spirit of the aforementioned work of Sugihara et al.[12] and construct a truncated model, which is affordable for the quantum chemical methods used here. Additionally, we construct point charge models for the solvated counter-ion, which facilitate the calculations considerably and take into account the electrostatic effect of the environment. This approach will be extended to an ab initio quantum mechanical/molecular mechanics (QM/MM) approach in which, for example, nonadiabatic "on-the-fly" surface hopping dynamics calculations[29] can be performed extending our current gas-phase approach for the formiminium and penta-3,5-dieniminium cations (see refs. [30, 31]).

The penta-3,5-dieniminium cation has been suggested by Garavelli et al.[32] as a minimum model for retinal photoisomerization. We construct our choice for model compounds by bracketing the above suggestion by using systems with one to four conjugated double bonds (formiminium cation up to hepta-3,5,7-trieniminium cation). This connects to our previous work on the photodynamics of the formiminium cation.[33,30] We decided to investigate the all-*trans* configurations of the PSBs because of their role in the photoisomerization in bR.

Computational Methods

The all-*trans* forms of the PSBs $CH_2NH_2^+$, $CH_2(CH)_2NH_2^+$, $CH_2(CH)_4NH_2^+$, $CH_2(CH)_6NH_2^+$ and of the SBs CH_2NH, $CH_2(CH)_2NH$, $CH_2(CH)_4NH$ and $CH_2(CH)_6NH$ are investigated. These compounds are referred to as PSB*n* or SB*n* depending on the number of double bonds *n* in the chain and according to the charge of the system. The calculations were carried out using two distinct modes: PSBs and SBs as isolated molecules and in interaction with counter-systems representing environmental effects. For the counter-system to the PSB 1) a single water molecule and 2) a complex consisting of formate surrounded by four water molecules, denoted as Fm4W, are chosen. The latter case simulates the Glu 113 environment in rhodopsin as modeled, for example, by Hufen at al.[13] and Asp 85 and Asp 212 in bR.[21] Proton transfer structures are obtained by considering the neutral SB in interaction with H_3O^+ and the complex formic acid and four waters (FA4W), respectively. In Figures 1 a–1 f investigated structures are illustrated for the largest compounds SB4 and PSB4.

Geometry optimizations and computation of vertical excitation energies are performed using DFT, TDDFT,[28,34,35] RI-CC2,[26,27,36] and MR-CISD methodologies. The TURBOMOLE program package[37] and the SVP[38] and aug-cc-pVDZ[39,40] basis sets were used for the TDDFT and RI-CC2 calculations. The functional B3LYP[41] was select-

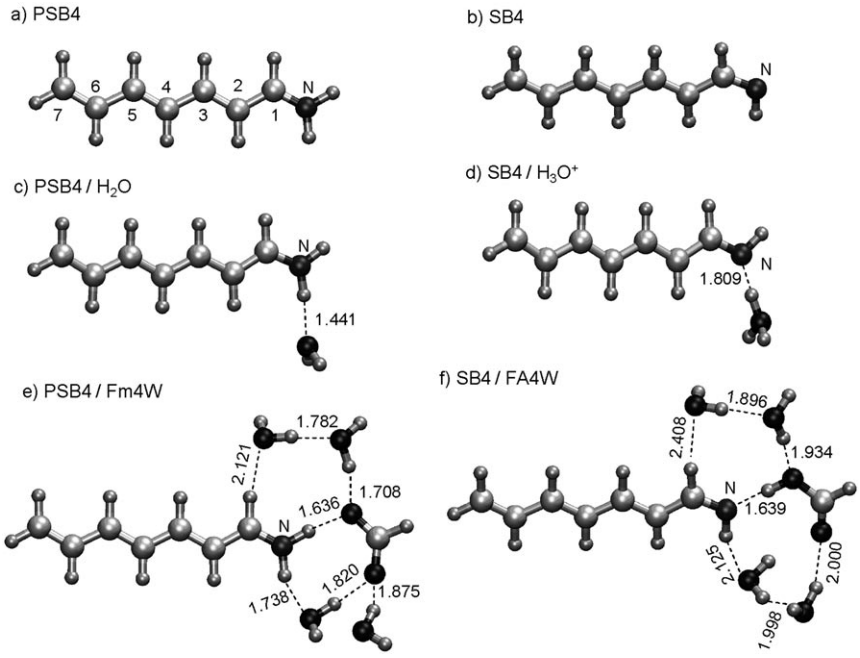

Figure 1. Isolated PSB4 and SB4 (a,b); PSB4 and SB4 in the presence of water and hydroxonium (c,d); PSB4 with Fm4W (e) and SB4 with FA4W (f). Bond distances are given in Å.

ed for the DFT and TDDFT calculations. The CASSCF and MR-CISD results were computed with the COLUMBUS package.[42–45] Size-extensivity corrections were taken into account by means of the extended Davidson correction[23,46,47] and are denoted by +Q. MR-CISD geometry optimizations are performed using the procedures described in refs. [23–25]. Atomic orbital (AO) integrals and AO gradient integrals have been computed with program modules taken from DALTON.[48]

Point charges are computed via the CHELPG[49] method for the ground states of the interaction complexes. The CHELPG charges for H_2O, H_3O^+, Fm4W and FA4W were used in subsequent point-charge model calculations treating only the PSB and SB, respectively, quantum mechanically. The internal coordinates describing the point charges and the distances to the chromophore were kept frozen. The calculation of the CHELPG charges were performed with the Gaussian program.[50]

For the computation of the vertical energies at the CASSCF and MR-CISD levels, the CAS has been constructed depending on the size of the system. For the SB1 and PSB1, a space with three orbitals (two π orbitals of a" symmetry and one a' symmetry orbital which is a lone pair orbital (n) in case of SBs and a σ orbital in case of PSBs) and four electrons [CAS-(4,3)] are used. Three states (ground state, $n\pi^*$ or $\sigma\pi^*$, and $\pi\pi^*$ states) are included in the state-averaging (SA) procedure at the CASSCF level (SA-3). A similar choice has been used previously for the calculation of the energy surfaces and conical intersections of PSB1.[30,33] For the SBn and PSBn ($n=3$, 5, and 7) systems, we have used a SA-4-CAS(6,5) space (four π orbitals and one n/σ orbital; ground state, $n\pi^*$ or $\sigma\pi^*$, and two $\pi\pi^*$ states). The reference space for the MR-CISD calculations is identical to the CAS space used in the CASSCF calculations. MR-CISD geometry optimizations have only been performed for the ground state and for the $\pi\pi^*$ state of the PSBn ($n=3$, 5, 7) series. Geometry optimizations of the $\pi\pi^*$ state (with and without the presence of point charges) were restricted to planar conformations. These geometry changes describe the initial phases of the photodynamics of PSB as has been described in ref. [51]. A SA-2-CASSCF(4,3) calculation (three π orbitals, ground state and lowest $\pi\pi^*$ state) is performed in the geometry optimizations. This CAS-(4,3) has also been used as a reference space for the MR-CISD calculations. The final expansion space in terms of configuration state functions (CSFs) for the MRCI calculations consists of the reference configurations and of all single and double excitations thereof into all internal and external orbitals. The interacting space restriction[52] was applied. The C and N 1s core orbitals were always kept frozen in the post-MCSCF calculations. For vertical excitation energies, calculations are performed with the aug-cc-pVDZ basis set for the SBn and PSBn systems $n=1$ and 2. The cc-pVDZ basis was used for $n=1$-4. For all geometry optimizations, the cc-pVDZ basis set without p-functions on the hydrogen atoms was used.

The Isolated PB and PSB Systems

Vertical Excitations

In Table 1 vertical excitation energies to the $1^1A''$, $2^1A'$ and $3^1A'$ states are displayed for the SBs and PSBs investigated in this work. In case of the SBs, these are the $n\pi_1^*$, $\pi_2\pi_1^*$ and $\pi_1\pi_1^*$ states, respectively, where π_2 denotes the highest occupied molecular orbital (HOMO), π_1 is HOMO-1 and π_1^* is the lowest unoccupied orbital (LUMO). For the PSBs the corresponding $\sigma\pi_1^*$, $\pi_2\pi_1^*$ and $\pi_1\pi_1^*$ states have been considered. The n and σ orbitals are predominantly localized on the nitrogen atom.

Table 1. Vertical excitation energies [eV] for neutral and protonated Schiff bases.[a]

	State	CASSCF	MRCI	MRCI+Q	RI-CC2	TDDFT
SB1[c]						
$1^1A''$	$n\pi^*$	5.47(5.66[b])	5.33(5.50[b])	5.26(5.42[b])	5.32	5.04
$2^1A'$	$\pi\pi^*$	10.46(11.45[b])	9.22(9.92[b])	8.78(9.44[b])	8.85	8.41
PSB1[c]						
1^1A_2	$\sigma\pi^*$	9.16(9.24[b])	8.62(8.74[b])	8.43(8.56[b])	8.46	7.79
2^1A_1	$\pi\pi^*$	10.29(10.47[b])	9.46(9.65[b])	9.18(9.40[b])	9.36	9.33
SB2[d]						
$1^1A''$	$n\pi_1^*$	5.17 (5.22[b])	5.03 (5.09[b])	4.95 (5.02[b])	5.02	4.55
$2^1A'$	$\pi_2\pi_1^*$	8.45 (8.85[b])	7.31 (7.61[b])	6.83 (7.14[b])	6.44	5.97
$3^1A'$	$\pi_1\pi_1^*,\pi_1^{*2}$	7.02 (6.96[b])	6.95 (7.00[b])	6.88 (6.98[b])	–	–
PSB2[d]						
$2^1A'$	$\pi_2\pi_1^*$	6.49 (6.60[b])	5.92 (6.03[b])	5.66 (5.79[b])	5.59	5.61
$1^1A''$	$\sigma\pi_1^*$	8.38 (8.38[b])	7.80 (7.78[b])	7.51 (7.50[b])	7.18	6.30
$3^1A'$	$\pi_1\pi_1^*,\pi_1^{*2}$	7.70 (7.74[b])	7.61 (7.63[b])	7.52 (7.54[b])	8.49	8.14
SB3[d]						
$1^1A''$	$n\pi_1^*$	5.03[b]	4.92[b]	4.85[b]	4.83	4.25
$2^1A'$	$\pi_2\pi_1^*$	7.29[b]	6.53[b]	6.19[b]	5.29	4.79
$3^1A'$	$\pi_1\pi_1^*,\pi_1^{*2}$	6.46[b]	6.35[b]	6.24[b]	–	5.98
PSB3[d]						
$2^1A'$	$\pi_2\pi_1^*$	5.64[b]	5.04[b]	4.73[b]	4.20	4.33
$3^1A'$	$\pi_1\pi_1^*,\pi_1^{*2}$	5.72[b]	5.65[b]	5.59[b]	6.25	5.92
$1^1A''$	$\sigma\pi_1^*$	7.86[b]	7.39[b]	7.15[b]	6.65	5.72
SB4[d]						
$1^1A''$	$n\pi_1^*$	4.95[b]	4.85[b]	4.79[b]	4.74	4.09
$2^1A'$	$\pi_2\pi_1^*,\pi_1^{*2}$	6.16[b]	5.59[b]	5.33[b]	4.56	4.07
$3^1A'$	$\pi_1\pi_1^*,\pi_2\pi_1^*$	5.97[b]	5.83[b]b	5.70[b]	5.85	5.03
PSB4[d]						
$2^1A'$	$\pi_2\pi_1^*$	5.08[b]	4.47[b]	4.14[b]	3.39	3.59
$3^1A'$	$\pi_1\pi_1^*,\pi_1^{*2}$	5.04[b]	4.90[b]	4.81[b]	5.26	4.84
$1^1A''$	$\sigma\pi_1^*$	7.68[b]	7.26[b]	7.05[b]	–	5.51

[a] aug-cc-pVDZ basis unless indicated. [b] cc-pVDZ basis. [c] SA-3-CAS(4,3) for CASSCF, MR-CI and MR-CI+Q. [d] SA-4-CAS(6,5) for CASSCF, MR-CI and MR-CI+Q.

Both, the $\pi_2\pi_1^*$ and $\pi_1\pi_1^*$ states show quite strong multireference character, partially due to the fact that the orbitals have been obtained by state-averaging and are not optimal for a specific state. For SB1 and PSB1 only the two lowest states are considered.

Comparison of MRCI and MRCI+Q results shows the usual reduction of a few tenths of an eV in excitation energies by the Davidson correction. Also as expected, SA-CASSCF excitation energies deviate in many cases significantly from the MRCI results. A characteristic feature of both SB and PSB systems is the relatively weak dependence of the energy of the $n\pi_1^*$ and $\sigma\pi_1^*$ states, respectively, on the chain length. This behavior can be explained by the localized character of the n and σ orbitals. In contrast, the two $\pi_2\pi_1^*$ and $\pi_1\pi_1^*$ excited states are stabilized strongly by extension of the chain length. For the SBs, the $n\pi_1^*$ state remains the lowest state over all the series of oligomers investigated. In case of the PSBs, the $\pi_2\pi_1^*$ state is already lower than the $\sigma\pi_1^*$ state starting for PSB2.

CASPT2 results obtained by Garavelli et al.[32] give an excitation of 4.12 eV for the $2^1A'(\pi\pi^*)$ state of PSB3. Cembran et al.[53] obtained 3.23 and 4.35 eV for the vertical excitation energies to the states $2^1A'$ and $3^1A'$ in the PSB4 system. The MR-CISD+Q results represent a significant improvement of the CASSCF data. However, we still observe a significant overestimation of the $\pi_2\pi_1^*$ excitation by the MR-CISD method. Much larger reference spaces would have to be employed as shown in previous investigations on butadiene.[54] Moreover, when comparing the above-mentioned CASPT2 results with the ones in this work, one should not forget that different basis sets (6-31G* in the former and cc-pVDZ in the latter) have been used. Both RI-CC2 and TDDFT methods give quite good results for the $\pi_2\pi_1^*$ state. However, the $3^1A'$ state having doubly excited character seems to be overestimated by both the RI-CC2 and TDDFT methods.

Geometry Relaxation in the $\pi_2\pi_1^*$ State

Geometry optimizations have been performed for planar geometries of the $\pi_2\pi_1^*$ state. This optimization characterizes the initial phase of the photoisomerization as has been discussed by Garavelli et al.[51] Therefore, it is of great interest to have accurate structural data available for the relaxed excited state of planar geometry in order to assess the validity of various computational methods. In Figure 2 CN and CC bond distances are displayed for the ground and $\pi_2\pi_1^*$ states of PSB4 and SB4. Comparing bond distances between the PSB and the SB for the ground state (see Figures 2a and 2c), a significant attenuation of the single/double bond alternation can be found as a consequence of the protonation. Similar results have been reported by Hufen et al.[14] Moreover, we observe good agreement between different computational methods. The situation is completely different for the $\pi_2\pi_1^*$ state of PSB4 (see Figure 2b). At CASSCF and MR-CISD levels, a main consequence of electronic excitation is a strong shortening of the C_1C_2 bond (nominally a single bond in the ground state) and a smaller, but significant stretching of the C_2C_3 bond. This stretching is

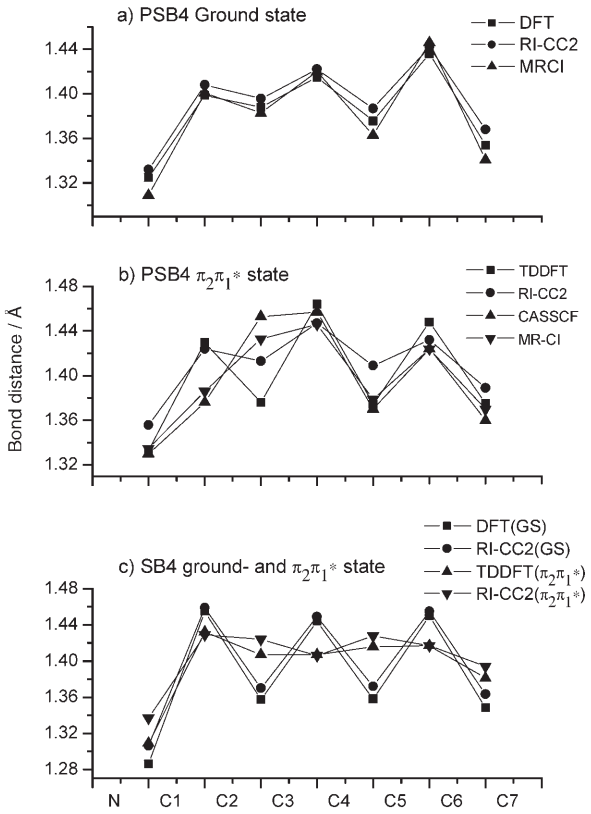

Figure 2. CN and CC bond lengths for isolated PSB4 in a) ground and b) $\pi_2\pi_1^*$ excited states, and c) for isolated SB4 in the $\pi_2\pi_1^*$ excited state.

slightly exaggerated at the CASSCF level. The C_2C_3 and C_3C_4 bond lengths are quite similar. Since these two bonds are the longest ones in the excited state, it is expected that the torsion around them is favored. At the B3LYP level, the C_2C_3 bond does not stretch and torsion would be disfavored. This finding is in good agreement with the work of Wanko et al.[10] where similar artifacts of the TDDFT/B3LYP approach are observed. The RI-CC2 method gives the C_2C_3 bond distance similar to the MR-CISD result. However, the C_1C_2 distance is too long.

Excited-State Proton Affinities

The proton affinity (PA) is defined as the energy balance of the reaction:

$$AH^+ \rightarrow A + H^+. \quad (1)$$

Table 2 shows the PAs of SBn ($n=1$–4) computed for the ground state and for the $2^1A'(\pi\pi^*)$ state. In the latter case vertical and adiabatic PAs are determined based on ground-state and planar optimized excited-state geometries, respectively. Zero-point corrections were not applied. Both for the ground- and excited states, the PAs increase with chain length. With some exceptions for SB1, the proton affinity is larger in the excited state than in the ground state by at least 10 kcal mol^{-1}. The effect of geometry relaxation (vertical vs adiabatic PAs) is small. For the ground state, computed PAs agree well between

Table 2. Vertical proton affinities [kcal mol^{-1}]. Adiabatic results are given in parentheses.

	State	CASSCF[a]	MRCI[a]	MRCI + Q[a]	B3LYP[b]	RI-CC2[b]
H_2O	GS	–	–	–	169.4	168.2
Fm	GS	–	–	–	344.0	344.9
Fm4W	GS	–	–	–	313.9	–
SB1	GS	218.5	219.6	219.2	214.4	212.3
	$2^1A'(\pi\pi^*)$	241.1	225.9	220.0	192.9	204.0
SB2	GS	225.6	230.1	230.5	228.6	225.1
	$2^1A'(\pi\pi^*)$	233.9	252.6	258.0	237.0(236.0)	243.9(244.7)
SB3	GS	239.1	239.9	239.0	238.3	233.4
	$2^1A'(\pi\pi^*)$	258.0	270.1	272.7	249.0(246.1)	257.6(254.8)
SB4	GS	247.0	246.5	244.9	245.1	238.3
	$2^1A'(\pi\pi^*)$	268.4	272.3	272.5	256.2(253.3)	265.2(261.4)

[a] SB1: SA-3-CAS(4,3)/cc-pVDZ; SB2, SB3, SB4: SA-4-CAS(6,5)/cc-pVDZ. [b] aug-cc-pVDZ basis.

the different methods. For the $2^1A'$ state B3LYP results are too small by approximately 10–20 kcal mol^{-1} as compared to the MR-CISD + Q results. Similar results for the ground-state PAs have been obtained by Zhou et al.[55] for SB2, SB3, SB4 and other SBs using the self-consistent charge, density-functional tight-binding method (SCC-DFTB) method.

Comparing the PAs of the SBs with those of the environmental model systems water, Fm and Fm4W given in Table 2, we see that protonation is significantly more favorable on the SB than on water. The reverse is true for Fm and Fm4W. Even though solvation effects represented by the four water molecules decrease the PA of Fm from 344 to 314 kcal mol^{-1}, this value is still significantly larger thaN the ~240 kcal mol^{-1} for SB4 in the ground state. Even though the PA of SB4 for the excited state is increased, it does not reach the Fm4W value.

Environmental Effects on SBs and PSBs

H_2O and H_3O^+

The PSB/H_2O and SB/H_3O^+ systems have been chosen because interactions with water molecules play an important role in biological systems and can serve as an interesting reference case. A more complex situation with a solvated formate group is discussed below. The geometry of the complex PSB4/H_2O is displayed in Figure 1c. The complex SB4/H_3O^+ resulting from intermolecular proton transfer is depicted in Figure 1d. As could already be seen in the discussion of Table 2, this latter complex cannot be expected to be stable. This has been confirmed by geometry optimizations where barrierless proton transfer to the SB is observed. In order to model the possible situation of a more complex situation with an energy barrier for proton transfer we kept the OH bond distance of H_3O^+ involved in the hydrogen bond constant at 0.983 Å and optimized the remaining coordinates only.

In Table 3 the optimized hydrogen bond (H-bond) distances are shown at RI-CC2 and TDDFT level for both types of complexes. In Table 4 respective interaction energies are given. In the ground state as well as in the excited state the H-bonds in the H_3O^+ complexes are clearly stronger than in the corresponding complexes with water. This can be seen from bond distances and interaction energies. Electronic excitation weakens the interaction in the PSB/H_2O cases but strengthens it for SB/H_3O^+. The weakening is in agreement with the migration of positive charge from the iminium side to the other end of the PSB due to the electronic excitation as reported by De Vico et al.[8] Similar charge shifts have also been observed in our MR-CISD calculations. A small shift of electron density toward the imine end (0.07 e_0) has been found in the $\pi_2\pi_1^*$ state of SBs as compared to the ground state, which is in line with the strengthening the SB/H_3O^+ interaction. Figure 3 shows the energetic situation for the SB4 system graphically. While for the situation of infinite separation of the proton transfer partners, SB4 + H_3O^+ is 70.1 kcal mol^{-1} (ground state,

Table 3. Computed N–H···O and N···H–O hydrogen bond distances [Å] in the ground and excited states of PSBn/H_2O and SBn/H_3O^+ complexes.

System	State	DFT/TDDFT	RI-CC2
		N–H···O	
PSB2/H_2O	GS	1.730	1.731
	$\pi_2\pi_1^*$	1.789	1.864
PSB3/H_2O	GS	1.780	1.774
	$\pi_2\pi_1^*$	1.814	1.858
PSB4/H_2O	GS	1.809	1.801
	$\pi_2\pi_1^*$	1.821	1.863
		N···H–O	
SB2/H_3O^+	GS	1.469	1.441
	$\pi_2\pi_1^*$	1.423	1.404
SB3/H_3O^+	GS	1.453	1.461
	$\pi_2\pi_1^*$	1.441	1.422
SB4/H_3O^+	GS	1.441	1.451
	$\pi_2\pi_1^*$	1.431	1.415

Table 4. Interaction energies [ΔE^a, kcal mol^{-1}] of PSBs and SBs with water and hydronium cation, respectively, using the aug-cc-pVDZ basis set. Values in parentheses are the energy differences between PBS/H_2O and SB/H_3O^+.

	State	ΔE^a	
		RI-CC2	DFT/TDDFT
PSB2/H_2O	GS	−17.6(−26.1)	−15.9(−28.2)
	$\pi_2\pi_1^*$	−16.3(−32.3)	−15.7(−28.4)
PSB3/H_2O	GS	−15.8(−31.3)	−13.7(−31.7)
	$\pi_2\pi_1^*$	−14.1(−37.0)	−13.4(−33.5)
PSB4/H_2O	GS	−14.5(−33.3)	−12.3(−34.6)
	$\pi_2\pi_1^*$	−12.9(−38.4)	−12.1(−35.7)
SB2/H_3O^+	GS	−48.4	−46.9
	$\pi_2\pi_1^*$	−60.5	−53.8
SB3/H_3O^+	GS	−48.7	−50.9
	$\pi_2\pi_1^*$	−63.8	−56.6
SB4/H_3O^+	GS	−51.3	−53.3
	$\pi_2\pi_1^*$	−67.7	−60.4

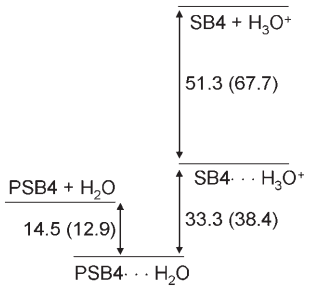

Figure 3. Proton transfer scheme for ground state and excited state (in parentheses) based on RI-CC2 results (energies in kcal mol^{-1}).

RI-CC2) higher in energy than PSB4 + H_2O, this energy difference decreases to 33.3 kcal mol^{-1} in the interacting complexes. Electronic excitation reduces this gap from 93.2 kcal mol^{-1} ($\pi_2\pi^*$ state, TDDFT) to 38.4 kcal mol^{-1} in the complexes.

$HCOO^-/(H_2O)_4$ and $HCOOH/(H_2O)_4$

Figures 1 e and 1 f show the complexes PSB4/Fm4W and the resulting intermolecular proton transfer structure SB4/FA4W. The choice of the system PSB4/Fm4W was inspired by the models for the retinal binding site used in the work of Sugihara et al.[12] and Hufen et al.[14] where the effect of the Glu 113 counterion has been taken into account together with water Wat2b molecule and Thr 94. We truncated the Glu 113 counterion to formate and included four water molecules (two for each oxygen). Geometry optimizations have been performed at the B3LYP/SVP level. The resulting hydrogen bond lengths computed for the ground state are given in Figures 1 e and 1 f. In analogy to the interaction with water, in case of SB/FA4W the OH distance of the carboxyl group has to be frozen (0.980 Å). In the TDDFT optimizations of the $\pi_2\pi_1^*$ excited state, problems were encountered with frequent root-flipping occurring with local excitations on the Fm4W subsystem. In order to overcome this problem, we froze the distance between the nitrogen and oxygen atoms from the Schiff base and formic acid/formate, respectively using a value of 2.675 Å taken as an average value from the ground state optimizations. Because of the size of the system, RI-CC2 calculations and the aug-cc-pVDZ basis set turned out to very demanding. Therefore, geometry optimizations for the complete system were carried out using the B3LYP/SVP approach. With this geometry, single-point calculations with the aug-cc-pVDZ approach were performed. In the next step a point-charge model was used and geometry optimizations at MR-CISD, CC2 and TDDFT levels were performed. Since no repulsive interaction terms with the PSB or SB partner were included in the point-charge model, all internal coordinates containing a point charge center were kept frozen.

Interaction energies computed for full systems without point charges are presented in Table 5 for the DFT/TDDFT methods. In case of PSBn/Fm4W interaction energies are significantly larger (around 100 kcal mol^{-1}) due to the ion-ion interaction as compared to the SBn/FA4W case (around 15 kcal mol^{-1}) where only neutral subsystems interact. As for the interaction with water (see Table 4), the strength of the interaction is reduced in the excited state. This reduction is here much larger (10-20 kcal mol^{-1}) as compared to the water case (around 1.5 kcal mol^{-1}, see Table 4). The relative stability of PSBn/Fm4W vs SBn/FA4W is dramatically affected by the interaction (see Table 5 and Figure 4). In the electronic ground state, the former system is more stable by ~10 kcal mol^{-1} than the latter. For $n=7$ both systems are practically isoenergetic in the excited state. As has already been discussed by Sugihara et al.[12] the strong interaction within the ion pair is a major factor explaining the stability of the PSB.

Table 5. Interaction energies [kcal mol^{-1}] of PSBs and SBs with Fm4W and FA4W, respectively, computed at the DFT/TDDFT/aug-cc-pVDZ level using DFT/TDDFT/SVP geometries. Values in parentheses are the energy differences between PBS/Fm4W and SB/FA4W.

System	State	DFT/TDDFT
PSB2/Fm4W	GS	−108.1 (−8.5)
	$\pi_2\pi_1^*$	−85.8 (6.1)
PSB3/Fm4W	GS	−100.0 (−9.5)
	$\pi_2\pi_1^*$	−89.9 (−6.3)
PSB4/Fm4W	GS	−94.5 (−10.5)
	$\pi_2\pi_1^*$	−75.8 (0.35)
SB2/FA4W	GS	−14.3
	$\pi_2\pi_1^*$	−13.9
SB3/FA4W	GS	−14.9
	$\pi_2\pi_1^*$	−15.9
SB4/FA4W	GS	−15.1
	$\pi_2\pi_1^*$	−15.5

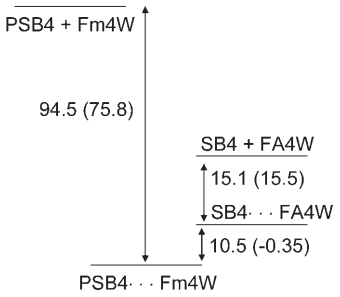

Figure 4. Proton transfer scheme for ground state and excited state (in parentheses) based on TDDFT/B3LYP results (energies in kcal mol^{-1}).

In Table 6 vertical excitation energies are presented for PSBs and SBs under the influence of the environmental point charge models Fm4W and FA4W, respectively. These data can be compared with the vertical excitation energies for isolated systems given in Table 1. A blue shift of ~0.6 eV is obtained for the $\pi_2\pi_1^*$ state of PSB4 with the MR-CI + Q and RI-CC2 methods. This is in the range of results obtained also by Wanko et al.;[11] 0.48 eV at the SORCI level and 0.71 eV using the CASPT2 approach.[15] However, we note that also the second π-excited state is blue-shifted as well by at least the same amount as the $\pi_2\pi_1^*$ state. This is consistent with a shift of electron density at the MR-CISD level toward the iminium end of PSB4, but in contrast to what is reported by Cembran et al.[15] where only a small blue shift of 0.1 eV has been found.

Table 6. Vertical excitation energies [eV] for neutral and protonated Schiff bases including point-charge model for FA4W and Fm4W. Energetic shift with respect to the isolated systems (Table 1) are given in parentheses.[a]

	State	CASSCF[b]	MRCI[b]	MRCI + Q[b]	RI-CC2[c]	TDDFT[c]
SB4/FA4W	$\pi_2\pi_1^*$,π_1^{*2}				4.52(−0.04)	4.04(−0.03)
	$\pi_1\pi_1^*$,$\pi_2\ \pi_1^2$				5.67(−0.18)	5.04(−0.01)
PSB4/Fm4W	$\pi_2\pi_1^*$	5.25(0.17)	4.89(0.42)	4.72(0.58)	4.04(0.65)	3.81(0.22)
	$\pi_1\pi_1^* + \pi_1^{*2}$	6.35(1.31)	6.02(1.12)	5.82(1.01)	5.79(0.53)	5.04(0.20)

[a] Ground state geometry optimized with inclusion of point charges. [b] SA-3-CAS(4,3)/cc-pVDZ (without p functions on H atoms). [c] aug-cc-pVDZ basis.

These differences would have nonnegligible consequences on the relative location and possible crossings between the two π-excited states induced by the environment. However, more investigations are required in order to substantiate these results for respective changes along the reaction path.

In Figure 5 CC and CN bond distances optimized for the SB4 and PSB4 point-charge complexes are plotted. In the ground state, the inclusion of the external field leads to an increase of the bond-alternation character (compare Figures 2a and 5a) due to a stronger localization of the positive charge on nitrogen. A similar effect has been observed by Sugihara et al.[56] In the ππ* state, the C_1C_2 bond is stretched at the MR-CISD level as compared to the isolated system (see Figures 2b and 5b) whereas the C_2C_3 and C_3C_4 bonds are shortened, leading to an approximate equalization of these three bonds. This would mean that torsions around the three bonds might occur in subsequent reaction steps. The CASSCF calculation predicts a maximum bond length at C_2C_3. It is noted that the TDDFT and CASSCF results are located almost symmetrically below and above the MR-CISD result for the C_1C_2 and C_2C_3 bonds. RI-CC2 is doing significantly better than TDDFT except for the distance C_1C_2.

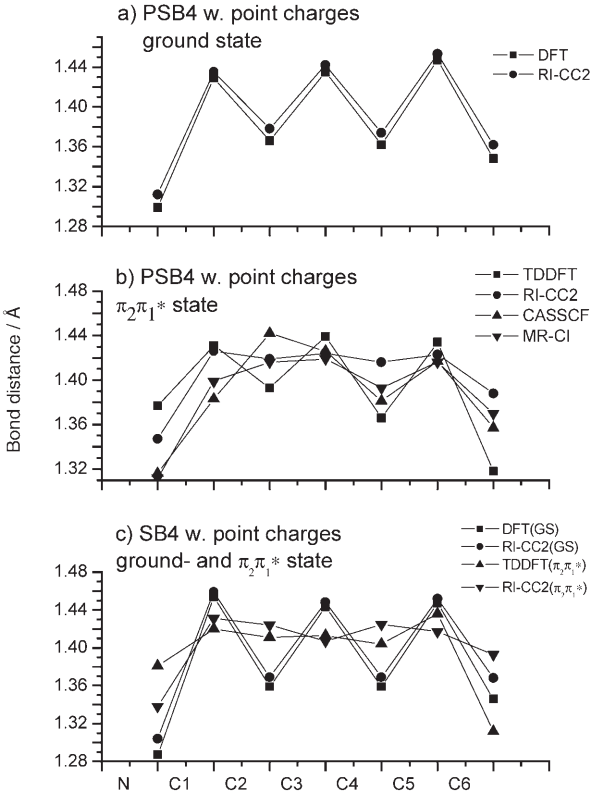

Figure 5. CN and CC bond lengths for PSB4 with Fm4W in a) ground and b) $\pi_2\pi_1^*$ excited states, and c) for SB4 with FA4W in the $\pi_2\pi_1^*$ excited state.

Conclusions

Systematic investigations on protonated Schiff bases have been performed with special emphasis on geometrical relaxation and environmental effects in electronically excited states. The aim of our research was twofold. On the one side different classes of computational methods (TDDFT, RI-CC2, CASSCF and MR-CISD) have been compared in order to assess the quality of these approaches particularly concerning excited-state geometry optimizations. By comparison of MR-CISD and CASSCF geometries it was found that the latter gave quite reliable results even though some overshooting of changes in bond lengths was observed. The TDDFT/B3LYP method does not qualify as a useful tool in this case since it shows strong bond-length alternation in the $\pi_2\pi_1^*$ state in strong contrast to CASSCF and MR-CISD results. This finding is in agreement with recent observations made by Wanko et al.[10] The RI-CC2 method shows significant improvements with respect to TDDFT/B3LYP, but is not satisfactory in all aspects. We plan to perform on-the-fly dynamic calculations in order to obtain better insight into the performance of the RI-CC2 method for geometry effects in the $\pi_2\pi_1^*$ state.

The other major goal of this work referred to environmental effects and to the energetics of proton transfer processes in this environment. Two models were selected: a water molecule and a hydrated formate molecular cluster. Proton transfer gave H_3O^+ and hydrated formic acid, respectively. The calculations show that also in the electronically excited state the interacting system has a large effect on the relative energies of the two proton transfer between PSB and SB. Similar effects have been observed by Sugihara et al.[12] for the ground state. Whereas in the ground state the system PSB4/hydrated formate is more stable than SB4/hydrated formic acid by ca. 10 kcal mol^{-1}, the stability difference is practically equal (even favoring slightly the side of SB4/hydrated formic acid) in the first excited state. This finding could have interesting consequences on the excited-state dynamics since not only *cis-trans* isomerization around a C=C bond could be observed but also strong vibrational activation of the NH bond in the iminium group depending on the barrier height along the proton trans-

fer path. Dynamic calculations are in preparation to get better insight into this question.

Acknowledgements

This work was supported by the Austrian Science Fund within the framework of the Special Research Program F16 (Advanced Light Sources) and Project P18411-N19. We are grateful for technical support and computer time at the Linux PC cluster Schrödinger III from the computer center of the University of Vienna.

Keywords: ab initio calculations · density functional calculations · excited states · proton transfer · Schiff bases

[1] I. Palings, J. A. Pardoen, E. van der Berge, C. Winkel, J. Lugtenburg, R. A. Mathies, *Biochemistry* **1987**, *26*, 2544.
[2] R. W. Schoenlein, L. A. Penteanu, R. A. Mathies, C. V. Shank, *Science* **1991**, *254*, 412.
[3] Q. Wang, R. W. Schoenlein, L. A. Penteanu, L. A. Penteanu, R. A. Mathies, C. V. Shank, *Science* **1994**, *266*, 422.
[4] J. Dobler, W. Zinth, K. Kaiser, D. Oesterhelt, *Chem. Phys. Lett.* **1996**, *261*, 389.
[5] G. Haran, K. Wynne, A. Xie, Q. He, M. Chance, R. M. Hochstrasser, *Chem. Phys. Lett.* **1988**, *144*, 215.
[6] St. L. Logunov, L. Song, M. El-Sayed, *J. Phys. Chem.* **1996**, *100*, 18586.
[7] R. González-Luque, M. Garavelli, F. Bernardi, M. Merchán, M. A. Robb, M. Olivucci, *Proc. Natl. Acad. Sci. USA* **2000**, *97*, 9379.
[8] L. De Vico, Ch. S. Page, M. Garavelli, F. Bernardi, R. Bassoni, M. Olivucci, *J. Am. Chem. Soc.* **2002**, *124*, 4124.
[9] F. Molnar, M. Ben-Nun, T. J. Martinez, K. Schulten, *J. Mol. Struct. (Theochem)* **2000**, *506*, 169.
[10] M. Wanko, M. Garavelli, F. Bernardi, T. A. Niehaus, T. Frauenheim, M. Elstner, *J. Chem. Phys.* **2004**, *120*, 1674.
[11] M. Wanko, M. Hoffmann, P. Strodel, A. Koslowski, W. Thiel, F. Neese, T. Frauenheim, M. Elstner, *J. Phys. Chem. B* **2005**, *109*, 3606.
[12] M. Sugihara, V. Buss, P. Entel, J. Hafner, *J. Phys. Chem. B* **2004**, *108*, 3673.
[13] J. Hufen, M. Sugihara, V. Buss, *J. Phys. Chem. B* **2004**, *108*, 20419.
[14] M. Schreiber, V. Buß, M. Sughihara, *J. Chem. Phys.* **2003**, *119*, 12045.
[15] A. Cembran, F. Bernardi, M. Olivucci, M. Garavelli, *J. Am. Chem. Soc.* **2004**, *126*, 16018.
[16] N. Ferre, M. Olivucci, *J. Am. Chem. Soc.* **2003**, *125*, 6868.
[17] T. Andruniów, N. Ferré, M. Olivucci, *Proc. Natl. Acad. Sci. USA* **2004**, *101*, 17908.
[18] U. F. Röhrig, L. Guidoni, U. Rothlisberger, *ChemPhysChem* **2005**, *6*, 1836.
[19] E. Tajkhorshid, J. Baudry, K. Schulten, S. Suhai, *Biophys. J.* **2000**, *78*, 683.
[20] U. F. Röhrig, L. Guidoni, A. Lalo, I. Frank, U. Rothlisberger, *J. Am. Chem. Soc.* **2004**, *126*, 15328.
[21] S. Hayashi, E. Tajkhorshid, K. Schulten, *Biophys. J.* **2002**, *83*, 1281.
[22] S. Hayashi, I. Ohmine, *J. Phys. Chem. B* **2000**, *104*, 10678.
[23] R. Shepard, H. Lischka, P. G. Szalay, T. Kovar, M. Ernzerhof, *J. Chem. Phys.* **1992**, *96*, 2085.
[24] R. Shepard in *Modern Electronic Structure Theory Part I* (Ed.: D. R. Yarkony), World Scientific, Singapore, **1995**, p. 345.
[25] H. Lischka, M. Dallos, R. Shepard, *Mol. Phys.* **2002**, *100*, 1647.
[26] A. Köhn, C. Hättig, *J. Chem. Phys.* **2003**, *119*, 5021.
[27] C. Hättig, *J. Chem. Phys.* **2003**, *118*, 7751.
[28] F. Furche, R. Ahlrichs, *J. Chem. Phys.* **2002**, *117*, 7433.
[29] J. C. Tully, *J. Chem. Phys.* **1990**, *93*, 1061.
[30] M. Barbatti, A. J. A. Aquino, H. Lischka, *Mol. Phys.* **2006**, *104*, 1053.
[31] M. Ruckenbauer, M. Barbatti, H. Lischka, unpublished results.
[32] M. Garavelli, P. Celani, F. Bernardi, M. A. Robb, M. Olivucci, *J. Am. Chem. Soc.* **1997**, *119*, 6891.
[33] H. Lischka, A. J. A. Aquino, M. Barbatti, M. Solimannejad, *Lecture Notes in Computer Science* **2005**, *3480*, 1004.
[34] R. Bauernschmitt, R. Ahlrichs, *Chem. Phys. Lett.* **1996**, *256*, 454.
[35] R. Bauernschmitt, M. Häser, O. Treutler, R. Ahlrichs *Chem. Phys. Lett.* **1997**, *264*, 573.
[36] F. Weigend, M. Häser, H. Patzelt, R. Ahlrichs, *Chem. Phys. Lett.* **1998**, *294*, 143.
[37] R. Ahlrichs, M. Bär, M. Häser, H. Horn, C. Kölmel, *Chem. Phys. Lett.* **1989**, *162*, 165.
[38] A. Schäfer, H. Horn, R. Ahlrichs, *J. Chem. Phys.* **1992**, *97*, 2571.
[39] T. H. Dunning, Jr., *J. Chem. Phys.* **1989**, *90*, 1007.
[40] R. A. Kendall, T. H. Dunning, Jr., R. J. Harrison, *J. Chem. Phys.* **1992**, *96*, 6769.
[41] A. D. Becke, *J. Chem. Phys.* **1993**, *98*, 5648.
[42] H. Lischka, R. Shepard, F. B. Brown, I. Shavitt, *Int. J. Quantum Chem. Quantum Chem. Symp.* **1981**, *15*, 91.
[43] R. Shepard, I. Shavitt, R. M. Pitzer, D. C. Comeau, M. Pepper, H. Lischka, P. Szalay, R. Ahlrichs, F. B. Brown, J. Zhao, *Int. J. Quantum Chem. Quantum Chem. Symp.* **1988**, *22*, 149.
[44] H. Lischka, R. Shepard, R. M. Pitzer, I. Shavitt, M. Dallos, Th. Müller, P. G. Szalay, M. Seth, G. S. Kedziora, S. Yabushita, Z. Zhang, *Phys. Chem. Chem. Phys.* **2001**, *3*, 664.
[45] H. Lischka, R. Shepard, I. Shavitt, R. M. Pitzer, M. Dallos, Th. Müller, P. G. Szalay, F. B. Brown, R. Ahlrichs, H. J. Böhm, A. Chang, D. C. Comeau, R. Gdanitz, H. Dachsel, C. Ehrhardt, M. Ernzerhof, P. Höchtl, S. Irle, G. Kedziora, T. Kovar, V. Parasuk, M. J. M. Pepper, P. Scharf, H. Schiffer, M. Schindler, M. Schüler, M. Seth, E. A. Stahlberg, J.-G. Zhao, S. Yabushita, Z. Zhang, COLUMBUS, an ab initio electronic structure program, **2004**, Release 5.9.
[46] S. R. Langhoff, E. R. Davidson, *Int. J. Quantum Chem.* **1974**, *8*, 61.
[47] P. J. Bruna, S. D. Peyerimhoff, R. J. Buenker, *Chem. Phys. Lett.* **1981**, *82*, 278.
[48] T. Helgaker, H. J. A. Jensen, P. Jørgensen, J. Olsen, K. Ruud, H. Ågren, T. Andersen, K. L. Bak, V. Bakken, O. Christiansen, P. Dahle, E. K. Dalskov, T. Enevoldsen, H. Heiberg, H.; Hettema, D. Jonsson, S. Kirpekar, R. Kobayashi, H. Koch, K. V. Mikkelsen, P. Norman, M. J. Packer, T. Saue, P. R. Taylor, O. Vahtras, DALTON, an ab initio electronic structure program, Release 1.0, **1997**.
[49] M. C. Breneman, K. B. Wiberg, *J. Comput. Chem.* **1990**, *11*, 361.
[50] Gaussian 03, Revision C.02, M. J. Frisch, G. W. Trucks, H. B. Schlegel, G. E. Scuseria, M. A. Robb, J. R. Cheeseman, J. A. Montgomery, Jr., T. Vreven, K. N. Kudin, J. C. Burant, J. M. Millam, S. S. Iyengar, J. Tomasi, V. Barone, B. Mennucci, M. Cossi, G. Scalmani, N. Rega, G. A. Petersson, H. Nakatsuji, M. Hada, M. Ehara, K. Toyota, R. Fukuda, J. Hasegawa, M. Ishida, T. Nakajima, Y. Honda, O. Kitao, H. Nakai, M. Klene, X. Li, J. E. Knox, H. P. Hratchian, J. B. Cross, V. Bakken, C. Adamo, J. Jaramillo, R. Gomperts, R. E. Stratmann, O. Yazyev, A. J. Austin, R. Cammi, C. Pomelli, J. W. Ochterski, P. Y. Ayala, K. Morokuma, G. A. Voth, P. Salvador, J. J. Dannenberg, V. G. Zakrzewski, S. Dapprich, A. D. Daniels, M. C. Strain, O. Farkas, D. K. Malick, A. D. Rabuck, K. Raghavachari, J. B. Foresman, J. V. Ortiz, Q. Cui, A. G. Baboul, S. Clifford, J. Cioslowski, B. B. Stefanov, G. Liu, A. Liashenko, P. Piskorz, I. Komaromi, R. L. Martin, D. J. Fox, T. Keith, M. A. Al-Laham, C. Y. Peng, A. Nanayakkara, M. Challacombe, P. M. W. Gill, B. Johnson, W. Chen, M. W. Wong, C. Gonzalez, J. A. Pople, Gaussian, Inc., Wallingford CT, **2004**.
[51] M. Garavelli, F. Bernardi, M. Olivucci, Th. Vreven, St. Klein, P. Celani, M. Robb, *Faraday Discuss.* **1998**, *110*, 51.
[52] A. Bunge, *J. Chem. Phys.* **1970**, *53*, 20.
[53] A. Cembran, F. Bernardi, M. Olivucci, M. Garavelli, *J. Am. Chem. Soc.* **2004**, *126*, 16018.
[54] M. Dallos, H. Lischka, *Theor. Chem. Acc.* **2004**, *112*, 16.
[55] H. Zhou, E. Tajkhorshid, T. Frauenheim, S. Suhai, M. Elstner *Chem. Phys.* **2002**, *277*, 91.
[56] M. Sugihara, V. Buss, P. Entel, M. Elstner, T. Frauenheim, *Biochemistry* **2002**, *41*, 15259.

Received: March 31, 2006
Revised: June 19, 2006
Published online on August 29, 2006

